PNAS RESEARCH ARTICLE | CELL BIOLOGY OPEN ACCESS

Induction of human trophoblast stem-like cells from primed pluripotent stem cells

Yu Jin Jang[a], Mijeong Kim[a], Bum-Kyu Lee[b], and Jonghwan Kim[a,1]

Edited by R. Roberts, University of Missouri, Columbia, MO; received August 25, 2021; accepted March 16, 2022

The placenta is a transient but important multifunctional organ crucial for healthy pregnancy for both mother and fetus. Nevertheless, limited access to human placenta samples and the paucity of a proper in vitro model system have hampered our understanding of the mechanisms underlying early human placental development and placenta-associated pregnancy complications. To overcome these constraints, we established a simple procedure with a short-term treatment of bone morphogenetic protein 4 (BMP4) in trophoblast stem cell culture medium (TSCM) to convert human primed pluripotent stem cells (PSCs) to trophoblast stem-like cells (TSLCs). These TSLCs show not only morphology and global gene expression profiles comparable to bona fide human trophoblast stem cells (TSCs) but also long-term self-renewal capacity with bipotency that allows the cells to differentiate into functional extravillous trophoblasts (EVT) and syncytiotrophoblasts (ST). These indicate that TSLCs are equivalent to genuine human TSCs. Our data suggest a straightforward approach to make human TSCs directly from preexisting primed PSCs and provide a valuable opportunity to study human placenta development and pathology from patients with placenta-related diseases.

human pluripotent stem cells | human trophoblast stem cells | trophoblast stem-like cells | primed pluripotency | BMP4

Significance

Treatment with bone morphogenetic protein 4 (BMP4) in human primed pluripotent stem cells (PSCs) for generating trophoblast lineage cells has sparked debate that the resulting cells are closer to amnion lineage cells rather than trophoblast. This study reports that trophoblast stem-like cells (TSLCs) can be generated from human primed PSCs by a short-term treatment of BMP4 without amnion lineage marker expression. In addition, we describe that TSLCs are self-renewing in long-term culture and bipotent as they can differentiate into functional extravillous trophoblasts and syncytiotrophoblasts. We propose an alternative method to generate an available model for studying human placental development from human primed PSCs.

The placenta is a temporary but pivotal organ that supports the fetus's growth during pregnancy by transporting nutrients and hormones, exchanging respiratory gases and waste, and conferring immunological protection (1). The human placenta originates from the trophectoderm, the outer layer of blastocyst, which develops into various specialized cell types including cytotrophoblasts (CT), syncytiotrophoblasts (ST), and extravillous trophoblasts (EVT) (2). Recently established human trophoblast stem cells (TSCs) possess an ability to differentiate into multiple cell types, such as multinucleated ST that are critical for gas/nutrient exchange as well as for metabolic and immunological functions and invasive EVT that migrate into the maternal uterus and modify its vessels to establish maternal blood flow into the placenta (3). Abnormal differentiation of trophoblasts and dysregulation in placental functions endangers the mother and fetus, leading to diverse pregnancy complications, such as preeclampsia, stillbirth, miscarriage, and intrauterine growth restriction (4). Notably, these disorders not only increase infant mortality and maternal morbidity but also impair the lifelong health of newborns (5). However, practical and ethical restrictions on accessing human placenta samples during pregnancy have greatly hindered precise understanding of the mechanisms underlying placenta development and placenta-associated complications.

Due to such limitations, animal models and in vitro placental cell lines derived from choriocarcinoma (6, 7) have been extensively used in the field. However, to fully understand the mechanisms underlying human placentation and placenta-related disorders, it is necessary to establish a reliable in vitro human model system that can mimic human placenta development. Although human TSCs have been successfully generated from both the blastocysts and CT from the first-trimester of placenta (3), from a clinical perspective, sourcing TSCs would not be straightforward due to ethical issues and health risks to both the mother and fetus when explanting placenta samples. As an alternative source of human TSCs, several attempts have been made to convert human pluripotent stem cells (PSCs) including embryonic stem cells (ESCs) and induced pluripotent stem cells (iPSCs) to trophoblast lineage cells using bone morphogenetic protein 4 (BMP4)-containing culture conditions (8–10). Although BMP4 treatment facilitates differentiation of human PSCs to trophoblasts (8–12), some reported that the BMP-treated cells often result in activation of mesendoderm or amnion markers (13–15) and a failure to establish long-term maintainable self-renewing bipotent cells. However, this view is controversial as other studies demonstrated that mesendoderm markers were not induced in the different culture compositions and substratum during

Author affiliations: [a]Department of Molecular Biosciences, The University of Texas at Austin, Austin, TX 78712; and [b]Department of Biomedical Sciences, Cancer Research Center, University at Albany, State University of New York, Rensselaer, NY 12144

Author contributions: J.K. designed research; Y.J.J. and M.K. performed research; Y.J.J., M.K., and B.-K.L. analyzed data; and Y.J.J., M.K., B.-K.L., and J.K. wrote the paper.

The authors declare no competing interest.

This article is a PNAS Direct Submission.

[1]To whom correspondence may be addressed. Email: jonghwankim@mail.utexas.edu.

This article contains supporting information online at http://www.pnas.org/lookup/suppl/doi:10.1073/pnas.2115709119/-/DCSupplemental.

Published May 10, 2022.

the induction of PSCs into trophoblast lineages (9, 16, 17). As for the activation of amnion markers in BMP-treated human primed PSCs (14, 15), it is still necessary to compare the amnion gene expression of TSC-like cells (TSLCs) induced from primed PSCs with that of bona fide amnion cells. This would determine whether the converted cells are truly amnion-like cells or not. Of note, several attempts (18–22) recently have been made to generate self-renewing human TSLCs from PSCs using human TSC culture medium (TSCM) (3). Recent papers reported that human PSCs can generate trophectoderm lineage stem cells under a micromesh culture condition (19) or chemically defined culture conditions (23). However, these methods lack functional validations of the derivatives (EVT and ST) from their trophectoderm lineage stem cells. Subsequent studies have reported that TSLCs can be generated from human naïve PSCs or expanded potential stem cells (EPSCs) (14, 15, 18, 20, 21). Most recently, a study showed that TSLCs can be derived from human primed PSCs under TSCM condition only, and 10 to 12 d of BMP4 treatment could enhance the conversion efficiency (22). Although it is unclear which protocol is better to generate functional TSLCs comparable to bona fide TSCs, all these reports provide valuable models to understand human trophoblast lineage development.

In this study, we successfully convert human primed PSCs to bipotent, self-renewing TSLCs that can differentiate into functional EVT and ST using TSCM together with transient treatment with BMP4. The resultant TSLC-derived EVT and ST express the representative marker genes, hormones, and transporters according to their respective lineages. Global transcriptome analysis and functional assays confirm high similarity between TSLCs and TSCs. In sum, we provide a simple, time- and cost-efficient method to directly convert human primed PSCs to TSLCs that are functionally equivalent to bona fide TSCs for another alternative in vitro placental model.

Results

Short-Term Treatment of BMP4 is Crucial to Generate Homogeneous and Long-Term Maintainable Human TSLCs from Primed PSCs. Multiple previous studies showed that the treatment of BMP4 or BAP (combination of BMP4, A83-01, and PD173074) can convert PSCs into trophoblast lineage cells (8–12, 24), indicating that BMP4 triggers trophoblast-specific gene expression programs. However, the BMP4- and BAP-treated cells were differentiated into heterogeneous cell populations that expressed ST- and EVT-specific marker and failed to acquire self-renewal capacity. In accordance with the previous observations, our continuous treatment of BMP4 or BAP to iPSCs (see *Materials and Methods*) resulted in mixed cell populations. In particular, the BMP4-treated cells start to die after 10 d of culture, indicating the loss of self-renewing ability (*SI Appendix*, Fig. S1*A*). Although the BAP-treated cells were more proliferative than the BMP4-treated cells, they did not show a typical morphology of TSCs (*SI Appendix*, Fig. S1*A*). The expression levels of TSC markers (TP63 and ELF5) were only 15 to 30% of the control TSCs in both BMP4- and BAP-treated cells, even though the expression levels were increased compared to undifferentiated iPSCs (*SI Appendix*, Fig. S1*B*). In addition, the BMP4-treated cells expressed a higher level of mesendoderm marker (T), while the BAP-treated cells did not up-regulate the expression of T (*SI Appendix*, Fig. S1*B*). Furthermore, while these cells expressed higher levels of HLA-G (EVT marker) and CGB (ST marker) than undifferentiated iPSCs as described previously (*SI Appendix*, Fig. S1*B*) (8, 9), the levels were significantly lower than those observed in EVT or ST differentiated from TSCs, suggesting that BMP4- and BAP-treated cells may not be able to fully differentiate into EVT or ST. With morphological heterogeneity observed in BMP4- and BAP-treated cells, all these results indicate that continuous treatment of BMP4 or BAP is not sufficient to generate a self-renewing population of TSLCs.

Since BMP4 was sufficient to trigger the loss of ESCs characteristics and induce trophoblast differentiation (8, 9), and TSCM maintains the self-renewal of TSCs in vitro (3), we subsequently tested continuous BMP4 treatment to the primed iPSCs in TSCM (TSCM-B-L) for 14 d with a control condition of TSCM alone (Fig. 1*A*). Cells cultured in TSCM-B-L condition showed polygonal morphology, which is a different morphology than bona fide TSCs. Meanwhile, cells cultured in TSCM showed only a few colony-forming cells as previously reported (21) (Fig. 1*B*). Accordingly, only a few TP63-expressing cells were observed in both conditions by immunofluorescent staining (Fig. 1*B*), and the transcript levels of ELF5 and TP63 in TSCM and TSCM-B-L conditions were lower than those in control TSCs (Fig. 1*C*). Notably, T, CXCR4, and HOXB1 (mesendoderm or mesoderm markers (25)) were highly expressed in the cells cultured in TSCM (Fig. 1*C* and *SI Appendix*, Fig. S1*D*), while ITGB6, GABRP, IGFBP3, VTCN1, and WNT6 [amnion markers (14, 21, 26–28)] were up-regulated in TSCM-B-L (Fig. 1*C* and *SI Appendix*, Fig. S1*C*). These indicate that continuous BMP4 treatment can induce amnion lineage markers in PSCs (14). We thought that long-term treatment of BMP4 may lead to adverse effects on attempts to generate TSLCs from PSCs. Since it has been reported that a transient exposure to BAP (24 to 36 h) can generate cell lines that are prone to differentiate into trophoblast lineage (29), we sought to test transient treatment of BMP4 in combination with TSCM. To optimize the duration of BMP4 treatment, we treated PSCs with BMP4 for 1, 2, 5, and 8 d (referred to as D1, D2, D5, and D8) and grew them for up to 14 d in TSCM after withdrawal of BMP4 (TSCM-B-S) (Fig. 1*A*). During BMP4 treatment, we changed media every day and split the cells when the confluency reached up to 80 to 90%. At 14 d, we examined the expression levels of TSCs and amnion markers using RT-qPCR. Regardless of the duration of BMP4 treatment, the resultant cells showed similar morphology and expression levels of TP63 and ELF5 with those of TSCs (Fig. 1 *D* and *E*). However, ITGB6, GABRP, IGFBP3, VTCN1, and WNT6 expression gradually increased with longer BMP4 treatment (Fig. 1*E* and *SI Appendix*, Fig. S1*E*), indicating that treatment of cells with BMP4 for more than 2 d might influence the expression of amnion genes during TSLCs conversion of PSCs. To verify the differentiation potential of TSLCs, we differentiated the cells into ST. Cells treated with BMP4 for 1 d did not develop cystic morphology, which is a key characteristic of ST, while cells treated with BMP4 for longer than 1 d were able to form a cystic shape during ST differentiation that was comparable to TSC-derived ST (Fig. 1 *F* and *G*). While the expression of ST markers CGB and SDC1 increased gradually with longer BMP4 treatment (Fig. 1*H*), ST derived from TSLCs treated with BMP4 for 2 d showed similar expression levels of ST marker genes to ST from TSCs. Considering marker gene expression, self-renewal, and differentiation potential, we finally selected 2 d BMP4 treatment as the best condition. These results demonstrate that 2 d of BMP4 treatment in TSCM is pivotal to convert human primed PSCs into proliferative TSLCs.

TSLCs Recapitulate the Hallmark Gene Expression of Bona Fide TSCs. To further validate our protocol and the authenticity of TSLCs, we generated TSLCs from iPSC (referred to here as

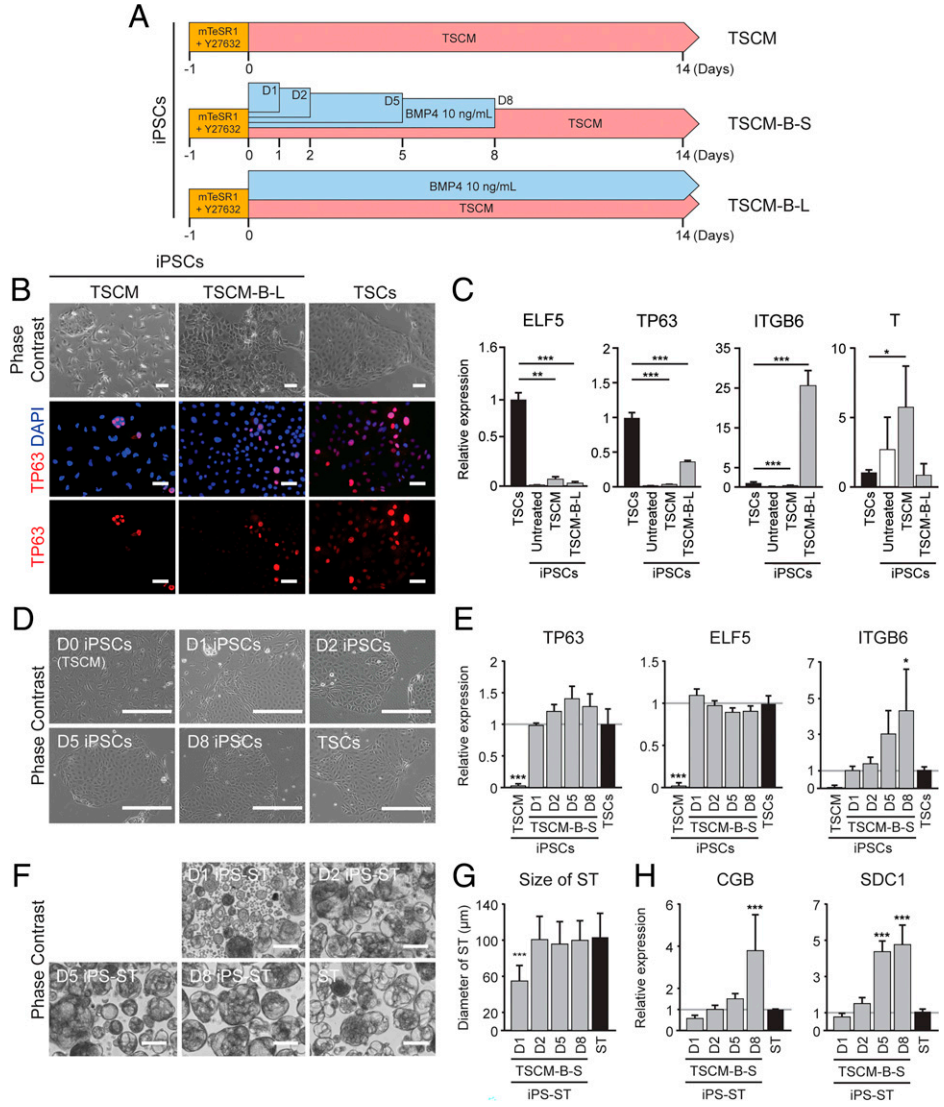

Fig. 1. Two days of BMP4 treatment with long-term culture in TSCM is sufficient to establish TSLCs from PSCs. (*A*) Schematic diagram of induction protocol. TSCM is used as a basal medium. There are three conditions tested to induce TSCs from human iPSCs. One is to culture the iPSCs in TSCM for over 14 d (TSCM), another is to culture the iPSCs in TSCM with BMP4 10 ng/mL for the first 1, 2, 5, or 8 d and replace TSCM without BMP4 (TSCM-B-S; D1, D2, D5, and D8), and the other is to culture the iPSCs in TSCM with BMP4 10 ng/mL for the entire duration (TSCM-B-L). (*B*) Representative phase contrast (*Top*) and immunofluorescent (IF) images (*Middle* and *Bottom*) of iPSCs cultured in TSCM or TSCM-B-L conditions and TSCs. Red indicates the protein expression of TP63. Blue (DAPI) indicates the nuclei. Overlayed images are shown in the *Middle*. Scale bars indicate 100 μm. (*C*) Relative transcript levels of TSCs (ELF5 and TP63), amnion (ITGB6), and mesendoderm (T) marker genes in the indicated cells. Error bars indicate SEM (biological repeats $n = 3$). Significance was indicated with $^{*}P < 0.05$, $^{**}P < 0.01$ and $^{***}P < 0.001$. (*D*) Representative phase contrast images of iPSCs cultured in TSCM or TSCM-B-S conditions (D1, D2, D5, and D8). TSCs were shown as a control. Scale bars indicate 400 μm. (*E*) Relative transcript levels of TSCs (TP63 and ELF5) and amnion (ITGB6) marker genes in the indicated conditions. Error bars indicate SEM (biological repeats $n = 4$). Significance was indicated with $^{*}P < 0.05$ and $^{***}P < 0.001$. (*F*) Representative phase contrast images of iPS-ST from the indicated conditions. The ST were differentiated from TSCs. Scale bars indicate 100 μm. (*G*) Bar graph showing diameter of 3D-cultured iPS-ST and ST from each condition. Error bars indicate SEM (biological repeats $n = 3$). Significance was indicated with $^{***}P < 0.001$. (*H*) Relative transcript levels of ST marker genes (CGB and SDC1) in the indicated conditions. Error bars indicate SEM (biological repeats $n = 3$). Significance was indicated with $^{***}P < 0.001$.

iPS-TSLCs) as well as ESCs (referred to here as ES-TSLCs) both of which were maintained under primed conditions, and then examined the levels of multiple marker genes of human TSCs. Both iPS- and ES-TSLCs demonstrated TSC-like morphology in shape (Fig. 2*A*), and they showed no detectable protein level of PSC core factor OCT4 and NANOG after the conversion, while having similar levels of TP63 and KRT7 expression as TSCs (Fig. 2*B* and *SI Appendix*, Fig. S2*A*). Moreover, the transcript levels of TSC-specific genes (ELF5, TFAP2C, HAVCR1, KRT7, TP63, and GATA3) were significantly induced comparable to those in TSCs, whereas they showed a significant reduction of POU5F1 and NANOG expression (Fig. 2*C*). We further tested the expression of TSC-specific microRNA clusters (miR-525-3p, miR-526b-3p, miR-517b-3p, and miR-517-5p) and methylation status of *ELF5* promoter region as previously suggested (30) and confirmed slightly lower but robust expression of the tested miRNAs in both iPS- and ES-TSLCs (Fig. 2*D*). Similar to TSCs, we also observed that the *ELF5* promoter in TSLCs was hypomethylated (Fig. 2*E*).

To further evaluate whether the TSLCs possess global gene expression signatures representative of TSCs, we performed global transcriptome analysis by RNA-sequencing. Principal component analysis (PCA) showed that iPS- and ES-TSLCs are clustered clearly with bona fide TSCs, suggesting that TSLCs and TSCs have a similar gene expression pattern. As expected,

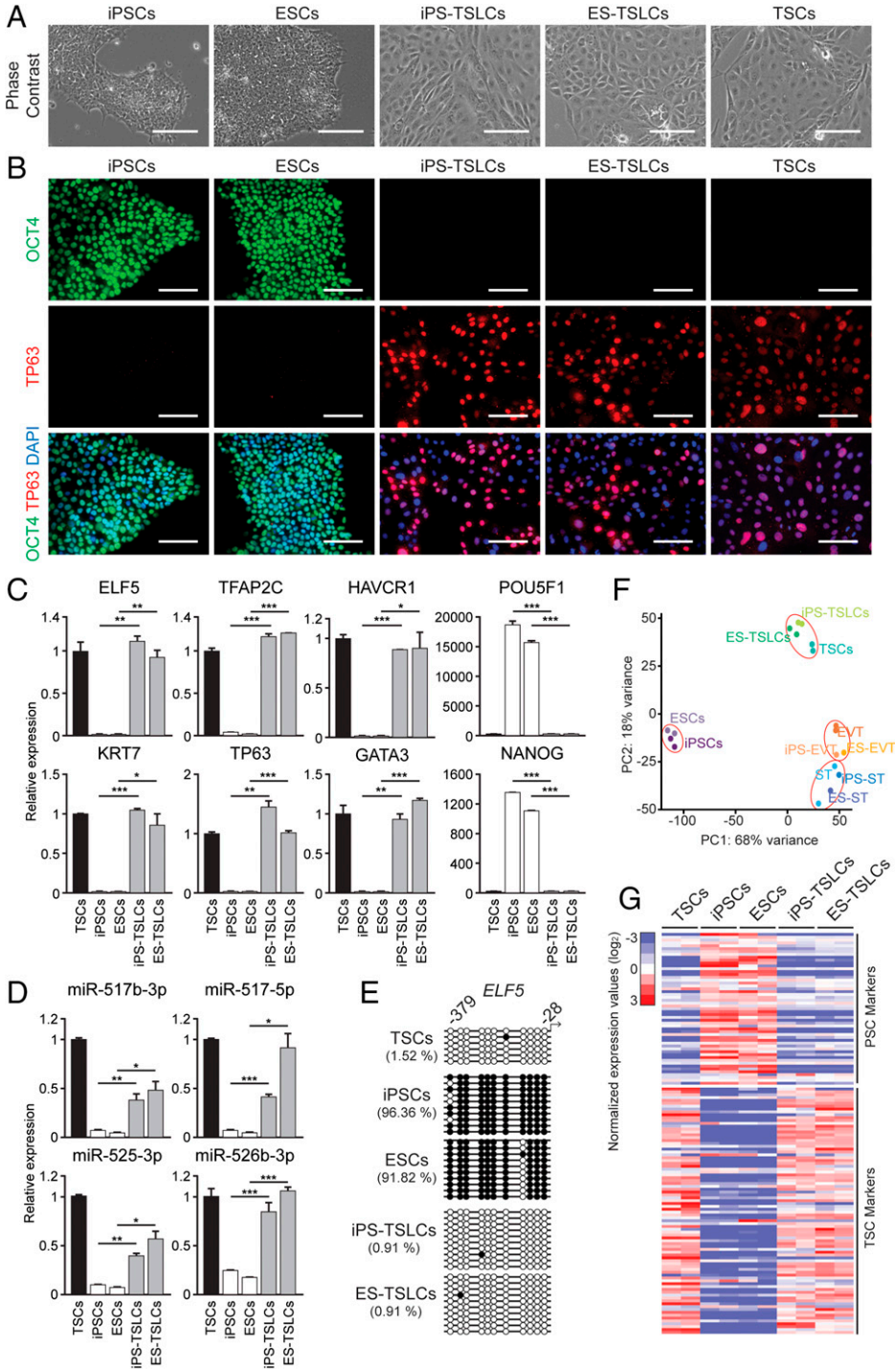

Fig. 2. TSLCs derived from primed iPSCs and ESCs show comparable gene expression signatures to TSCs. (*A*) Representative phase contrast images of iPSCs, ESCs (H9), iPS-TSLCs, ES-TSLCs, and control TSCs. Scale bars indicate 100 μm; all images taken at the same magnification. (*B*) Immunofluorescent (IF) staining images showing the protein expression of PSC marker OCT4 (green, *Top*) and TSC marker TP63 (red, *Middle*) in the indicated cell types. Overlayed images of OCT4 and TP63 are shown in the *Bottom* with the nuclei staining with DAPI (blue). Scale bars indicate 100 μm. (*C* and *D*) Relative transcript levels of TSC markers (ELF5, TFAP2C, HAVCR1, KRT7, TP63, and GATA3) and PSC markers (POU5F1 and NANOG) (*C*) and TSC-specific miRNA clusters (miR-525-3p, miR-526b-3p, miR-517b-3p, and miR-517-5p) (*D*) in the indicated cell types. Error bars indicate SEM (biological repeats $n = 3$). Significance was indicated with **P* value < 0.05, ***P* value < 0.01, and ****P* value < 0.001. (*E*) Distribution of methylated CpG sites (filled circles) at the *ELF5* promoter in the indicated cell types. The relative percentage of methylated CpG sites is indicated with cell types. (*F*) PCA for gene expression of the indicated cell types. Each dot is one biological replicate. (*G*) A heatmap showing normalized relative expression of PSC (31) and TSC markers (21) (Dataset S1) in the indicated cell types indicated. *y* axis shows representative PSC and TSC markers. Each cell type is represented by 2 biological replicates in each column. Relative expression was calculated by dividing the level of a gene with average gene expression of all cell types.

the cluster containing TSLCs and TSCs was separated from PSCs, EVT, and ST (Fig. 2*F*). Next, we confirmed that compared to PSCs, the levels of PSC-specific genes (31) were lower in iPS-TSLCs and ES-TSLCs, while the levels of TSC-specific genes (21) were comparable to the levels in TSCs, which further evinces proper derivation of TSLCs from PSCs (Fig. 2*G* and Dataset S1). Since previous papers have shown that human primed PSCs differentiate into mesendoderm (or mesoderm) or

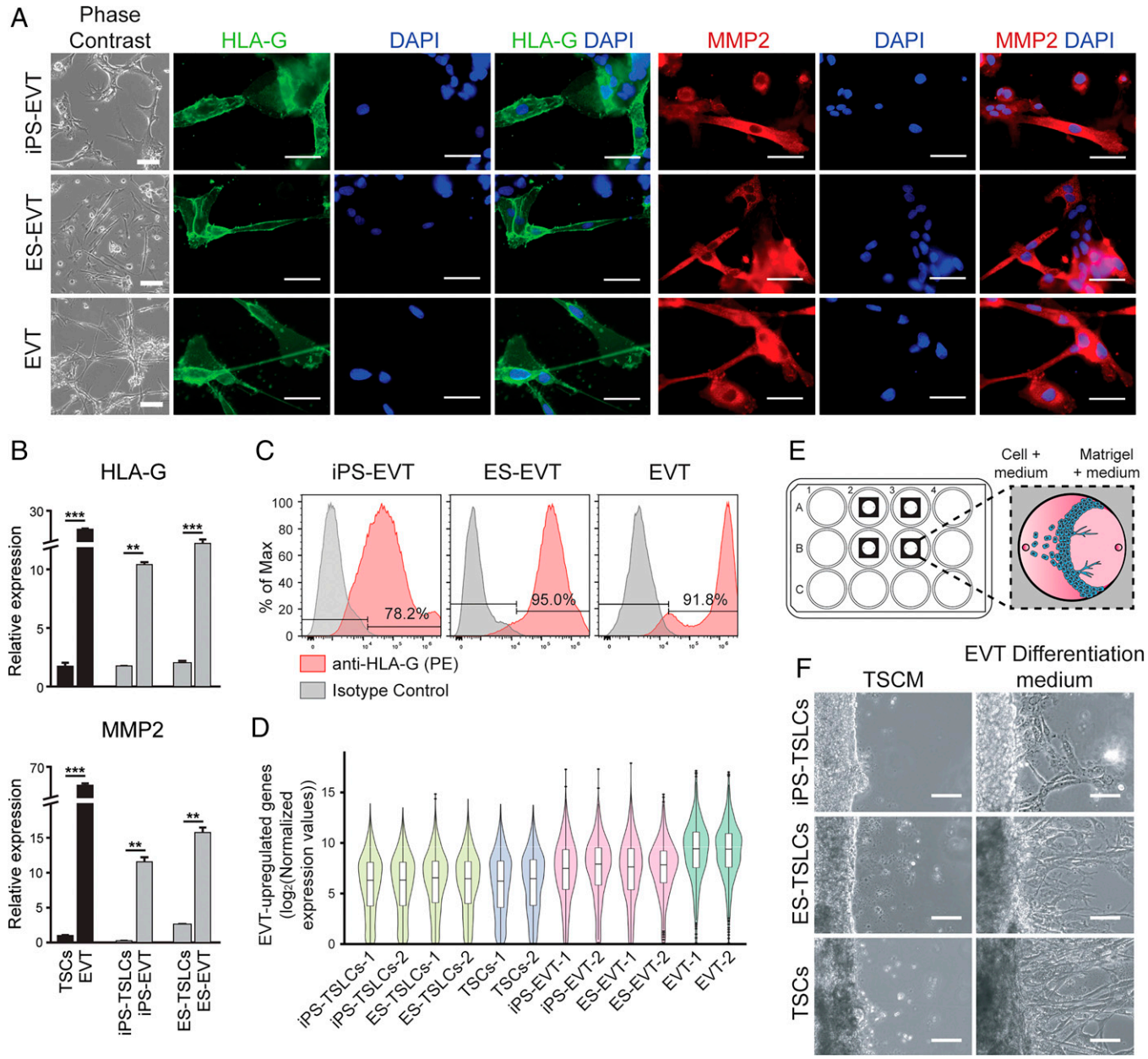

Fig. 3. TSLCs can differentiate into EVT-like cells. (*A*) Representative phase contrast (*Left*) and immunofluorescent (IF) images of indicated cell types. Green indicates the protein expression of HLA-G. Red indicates the protein expression of MMP2. Blue (DAPI) indicates nuclei. Overlayed images are shown on the *Right*. Scale bars indicate 100 μm. (*B*) Relative transcript levels of EVT marker genes (HLA-G and MMP2) in indicated cell types to control TSCs. Error bars indicate SEM (biological repeats $n = 3$). Significance was indicated with $^{**}P < 0.01$ and $^{***}P < 0.001$. (*C*) Flow cytometry analysis of surface HLA-G expression was performed with iPSC-EVT, ES-EVT, and EVT at 8 d, which were differentiated from iPS-TSLCs, ES-TSLCs, and TSCs. The expression was compared with an isotype control of each cell type. (*D*) Violin plots showing the expression distribution of 833 EVT-up-regulated genes (3) (Dataset S2) in the indicated cell types. The box indicates 25th, 50th, and 75th percentiles. (*E*) Schematic illustration of imaging chamber (32). Imaging chambers were adhered to the bottom of a 12-well plate. The Matrigel and medium (TSCM or EVT differentiation medium) mix was added to one of the open ports and allowed to equilibrate at 37 °C. After 1 h, the TSLCs or TSCs were seeded into another port with 30 μL of TSCM or EVT differentiation medium. One milliliter of TSCM or EVT differentiation medium was added to each well. (*F*) Representative phase contrast images of invading cells in TSCM or EVT differentiation medium at 8 d. Scale bars indicate 100 μm.

amnion-like cells upon BMP treatment (13–15), we also monitored the levels of mesendoderm marker genes as well as amnion-up-regulated genes, which are predominantly expressed in human amnion at 9 gestational weeks (26). The expression levels of mesendoderm marker genes (T, MIXL1, EOMES, PDGRFA, CXCR4, HOXB1, TBX6, VCAM1, and LMO2) (25) in TSLCs were lower than those in PSCs and comparable to their levels in control TSCs (*SI Appendix*, Fig. S1*F* and Table S3). In contrast with the human amnion tissue (26), iPS- and ES-TSLCs showed similar expression levels of amnion genes to genuine TSCs (*SI Appendix*, Fig. S2 *B* and *F* and Dataset S1), suggesting that our protocol did not promote PSCs to differentiate into amnion. Moreover, we confirmed that both TSLC lines can self-renew for over 20 passages without losing typical TSC morphology and proliferation capacity (*SI Appendix*, Fig. S2 *C* and *D*). Consistent with the morphology, the levels of TP63, ELF5, KRT7, TFAP2C, and EGFR were stably maintained in both iPS-TSLCs and ES-TSLCs even after 20 passages, and >90% of TSLCs showed KRT7 and GATA3 expression (*SI Appendix*, Fig. S2 *E* and *G*), suggesting these cells can self-renew for a long time. In summary, all these results further support that the TSLCs we generated are similar to bona fide TSCs.

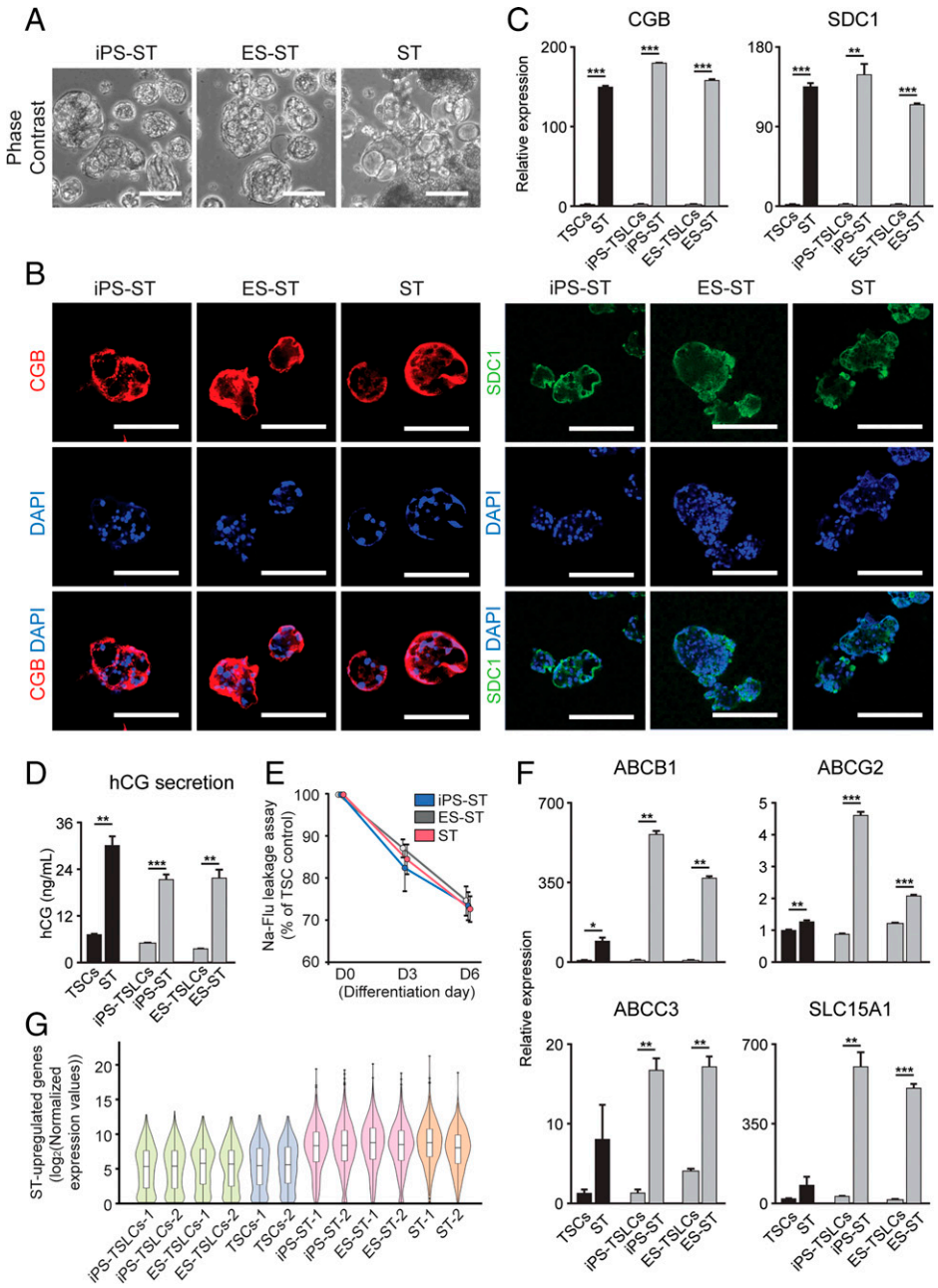

Fig. 4. TSLCs can differentiate into ST-like cells. (*A*) Representative phase contrast of indicated cell types. Scale bars indicate 100 μm. (*B*) Representative immunofluorescent (IF) images of indicated cell types. Red indicates the protein expression of CGB. Green indicates the protein expression of SDC1. Blue (DAPI) indicates the nuclei. Overlayed images are shown at *Bottom*. Scale bars indicate 100 μm. (*C*) Relative transcript levels of ST marker genes (CGB and SDC1) in indicated cell types to control TSCs. Error bars indicate SEM (biological repeats $n = 3$). Significance was indicated with $^{**}P < 0.01$ and $^{***}P < 0.001$. (*D*) The protein level of secreted hCG in indicated cell types. Error bars indicate SEM (biological repeats $n = 3$). Significance was indicated with $^{**}P < 0.01$ and $^{***}P < 0.001$. (*E*) Leakage of sodium fluorescein (Na-Flu) through iPS-ST, ES-ST, and ST differentiated on 3 d and 6 d post seeding. Data are presented as mean ± SD for 5 biological repeats and calculated as % of each 0 d control. (*F*) Relative transcript levels of multiple ABC transporters (ABCB1, ABCG2, and ABCC3) and carrier transporter (SLC15A1) in indicated cell types to control TSCs. Error bars indicate SEM (biological repeats $n = 3$). Significance was indicated with $^{*}P < 0.05$, $^{**}P < 0.01$ and $^{***}P < 0.001$. (*G*) Violin plots showing the expression distribution of 911 ST-up-regulated genes (3) (Dataset S3) in the indicated cell types. The box indicates 25th, 50th, and 75th percentiles.

TSLCs can differentiate into functional EVT. Since genuine TSCs can differentiate into both EVT and ST (3), we examined the differentiation potential of our TSLCs generated from primed PSCs. After EVT differentiation, both iPS-TSLC-derived EVT (iPS-EVT) and ES-TSLC-derived EVT (ES-EVT) showed primary EVT features of spindly, elongated cell morphology comparable to the control EVT derived from TSCs (Fig. 3*A*). Consistently, iPS- and ES-EVT showed robust expression of EVT-specific markers of HLA-G and MMP2 in both transcript and protein levels (Fig. 3 *A* and *B*). We assessed the surface expression of HLA-G in EVT differentiated from iPS-TSLCs, ES-TSLCs, and TSCs using flow cytometry. Although the intensity of fluorescence signals varied between cells, 78.2% of iPS-EVT and 95.0% of ES-EVT expressed HLA-G in comparison with 91.8% of EVT differentiated from TSCs (Fig. 3*C*). Next, we performed transcriptome analysis to compare EVT-up-regulated gene expression patterns between TSLC-derived EVT and EVT. We observed that 833 EVT-up-regulated genes, obtained by comparing TSCs with EVT from published data (3), were indeed activated in TSLC-derived

EVT compared to undifferentiated TSLCs (Fig. 3*D* and Dataset S2). Likewise, PCA of gene expression showed EVT and TSLC-derived EVT clustered together but well-separated from TSLCs (Fig. 2*F*). Since EVT invasion into the maternal decidua is a crucial step to anchor the placenta to the uterus and establish maternal blood flow into the placenta, invasion ability is a signature characteristic of EVT. To functionally validate invasion ability, we differentiated both TSLCs into EVT in Matrigel-blocked chambers (32) (Fig. 3*E*). Although the invasion efficiency of EVT from TSLCs (especially iPS-TSLCs) seemed slightly lower than EVT derived from control TSCs, their ability to invade the Matrigel region is clear and evident compared to an undifferentiated control (Fig. 3*F*). These results demonstrate that primed PSC-derived TSLCs differentiate into functional EVT comparable to bona fide EVT.

TSLCs can Differentiate into Functional ST. We also tested the differentiation potential of TSLCs toward ST. After ST differentiation, both iPS-TSLC-derived ST (iPS-ST) and ES-TSLC-derived ST (ES-ST) exhibited a cystic morphology that is a key characteristic of ST grown in three-dimensional (3D) culture in conjunction with a robust level of CGB and SDC1 protein confirmed by immunofluorescent staining (Fig. 4 *A* and *B*). We also confirmed the induction of CGB and SDC1 in transcript levels, both of which are well-known markers for ST subpopulations (3, 33, 34) (Fig. 4*C*). More importantly, as ST secrete human chorionic gonadotropin (hCG) into the maternal blood (35), we verified by enzyme-linked immunosorbent assay (ELISA) that our TSLC-derived ST secrete hCG significantly higher than TSLCs, reflecting the endocrinological capabilities of iPS-ST and ES-ST (Fig. 4*D*). One of the main functions of placenta is acting as a barrier at the maternal-fetal interface, and ST is a major cell type composing that barrier. We evaluated whether TSLC-derived ST can function as a barrier by conducting the apical-to-basal leakage of sodium fluorescein (Na-Flu) assay (36). iPS-TSLCs, ES-TSLCs, and control TSCs were seeded in the apical chamber of transwell and cultured for 6 d in ST differentiation conditions. At 3 d and 6 d, the medium in the apical chamber was replaced with Na-Flu containing culture medium, and the cells were incubated for 1 h. To assess the role of the placental barrier in ST, we transferred the medium from the basal chamber to a 96-well plate and measured the levels of fluorescence. All tested cells showed similar reduction of the Na-Flu leakage at 6 d, indicating that the ST derived from both iPS-TSLCs and ES-TSLCs can form a cellular barrier much like ST differentiated from genuine TSCs (Fig. 4*E*). ST also play an important role in active transport in the placenta by expressing various receptors and transporters (37, 38). In agreement with the previous report (24), the expression of transport-related genes, such as ABCB1 and ABCG2 [drug transporters in the placenta (39)], ABCC3 [ABC transporter in the placenta (40), and SLC15A1 [a solute carrier (41)] were elevated in both iPS- and ES-ST (Fig. 4*F*). In the global transcriptome analysis, PCA showed that TSLC-derived ST clustered with ST (Fig. 2*F*). Additionally, we further confirmed that ST differentiated from ES- and iPS-TSLCs showed increased expression of 911 ST-up-regulated genes obtained by comparing TSCs derived from CT with ST from published data (3) (Fig. 4*G* and Dataset S3). Taken all together, these results demonstrate that the TSLCs generated from primed PSCs harbor bipotency, a core characteristic of TSCs.

Discussion

Due to the difficulty and ethical issues of studying the human placenta in vivo as well as the unique aspects of human pregnancy compared to other mammals, it is imperative to develop a genetically tractable in vitro model of human placenta development (42). In this study, we successfully generated human TSLCs derived from human primed PSCs by optimizing the duration of BMP4 treatment in TSCM. We verified that these TSLCs can self-renew for a long period of time and have bipotency with which the cells can differentiate into EVT and ST. We have shown the global gene expression profiles of TSLCs, TSLC-derived EVT, and TSLC-derived ST were similar to those of human TSCs, EVT, and ST, respectively. We verified the expression of trophoblast-specific miRNA and hypomethylation of *ELF5* promoter in TSLCs. All these results indicate that these TSLCs accurately recapitulate two key features of TSCs, such as self-renewal and bipotency.

Multiple groups have also attempted to derive trophoblast lineage cells from human PSCs using BMP4 for the entire culture (8, 9, 24). However, prior reports have mostly focused on the expression of differentiated cell markers, such as HLA-G or CGB, rather than those that typify stem cell properties. Although one group generated CT-like stem cells from human PSCs that express CDX2 and TP63 and confirmed that the resultant cells can be differentiated into ST-like and EVT-like cells based on the marker gene expression, invasion capacity, and hormone production, these cells do not efficiently self-renew, and the authors did not test directed differentiation into ST or EVT (10). In accordance with this observation, we also confirmed that TSLCs generated by previously reported protocols undergo cell death after several passages, indicating they may not be suitable for long-term culture. In contrast, our TSLCs can be stably maintained without the loss of typical morphology of TSCs and key marker gene expression, indicating that we established a more selective and reliable method for deriving TSLCs from human primed PSCs.

Recently, two studies reported bipotent trophoblast-like stem cells derived from primed PSCs by micromesh and chemically defined culture medium, respectively (19, 23). Additionally, there are multiple paths for deriving human TSCs from naïve ESCs (14, 15, 20, 21) and reprogramming of somatic cells (43, 44). Although these groups used different protocols for inducing trophoblast lineage cells from different cell sources, they showed that the induced cells exhibit typical characteristics of TSCs. Further systematic evaluation of the established cells and the culture protocols will be critical for developing comprehensive in vitro placenta models.

Very recently, Wei et al., (22) showed that primed PSCs convert to TSLCs under TSCM condition. They also showed that 10–12 d of BMP4 treatment could enhance the conversion process. This group isolated and expanded TSC-shaped colonies formed under TSCM alone with very low efficiency, which we also showed in Fig. 1*B*. Although 10 to 12 d of BMP4 treatment increased the conversion, the resultant cells showed a lower efficiency of EVT differentiation based on HLA-G expression (22). Interestingly, in our hands, longer BMP4 treatment gradually increased the expression of amnion genes (Fig. 1E and *SI Appendix*, Fig. S1*E*), suggesting that the precise duration of BMP4 treatment might be critical for bipotency of the resultant TSLCs.

Previous studies on inducing trophoblast lineage from human PSCs have resulted in different outcomes in some cases. Recently, two studies claimed that BMP-treated PSCs differentiated into amnion-like cells (14, 15). However, although we also used BMP4, our TSLCs showed a similar global expression profile to that of bona fide TSCs and exhibited significantly lower amnion gene expression than human amnion tissue (26)

(Fig. 2*G* and *SI Appendix*, Fig. S2 *B* and *F* and Table S3). We applied two modifications to our protocol. First, the duration of BMP4 treatment was shorter in our study. Since we observed gradual activation of the amnion genes upon longer BMP4 treatment (Fig. 1*E* and *SI Appendix*, Fig. S1*E*), we optimized our protocol by treating BMP4 for 2 d. Additionally, we used previously defined TSCM (3) in combination with the BMP4 treatment. With these, we found that our TSLCs have TSC-specific gene expression patterns comparable to TSCs rather than induced amnion-like gene expression patterns (Fig. 2*G* and *SI Appendix*, Fig. S2 *B* and *F* and Table S3). We report the simple and reliable protocol to convert human primed PSCs into TSLCs similar to TSCs, rather than amnion-like cells.

The ST plays important roles in metabolic activity of placenta by directly contacting with maternal blood, secreting hormones, and transporting nutrients for the fetus (45). Aberrancy in trophoblast lineage specification toward the ST may cause abnormal placental functions (46). As one of the essential characteristics of ST is the expression of various drug transporters that may protect the fetus from xenobiotics, an appropriate in vitro placental model could be used for studying placental functions such as the regulation of drug transporters. Similar to the previous study (24), we confirmed that TSLC-derived STs expressed multiple ABC transporters and carrier transporters, suggesting they can serve as a valuable model system to study placental transport and metabolic activity.

Notably, to define the characteristics of human trophoblast cells generated from various sources, a previous report suggested four criteria: a set of marker expression (KRT7, TFAP2C, and GATA3), HLA class I expression, methylation of ELF5 promoter, and expression of microRNAs (miRNAs) from chromosome 19 miRNA cluster (C19MC) (30). Among these four criteria, our TSLCs satisfied three criteria but expressed the HLA class I gene (HLA-A) (*SI Appendix*, Fig. S3*A*), which is a similar level to the bona fide TSCs derived from a human blastocyst (*SI Appendix*, Fig. S3*A*) (3). The similarities and differences observed in the trophoblast cells generated from different cell sources might be of interest for the future applications of these cells.

In summary, we have demonstrated that self-renewing and bipotent human TSLCs can be derived from human primed ESCs and iPSCs. These TSLCs can serve as a useful in vitro model system to investigate the placental barrier, development, and cell-based pharmacological screening for the transfer and biological effects of pathogens, drugs, or toxins.

Materials and Methods

Cell Culture. Human PSCs (Yamanaka retrovirus reprogrammed human iPSCs, ACS-1023, ATCC and human ESCs, H9, WiCell) were maintained on Matrigel (Corning)-coated plates with mTeSR1 medium (Stemcell Technologies). When the cells reached about 70 to 80% confluence, they were passaged with ReLeSR (Stemcell Technologies) according to the manufacturer's protocol, at a 1:10 ratio. Human TSCs obtained from Dr. Takahiro Arima (CT27 derived from CT isolated from the first trimester human placenta) were cultured as previously described (3). Briefly, the TSCs were plated on 5 μg/mL collagen IV (Corning)-coated dishes with TSCM (Dulbecco's modified Eagle medium/nutrient Mixture F-12 [DMEM/F12; Gibco]) medium supplemented with 1% ITS-X supplement (Gibco), 0.5% penicillin-streptomycin (Gibco), 0.3% bovine serum albumin (BSA; Sigma-Aldrich), 0.2% fetal bovine serum (FBS; GeminiBio), 0.1 mM β-mercaptoethanol (Sigma-Aldrich), 0.5 μM A83-01 (Wako Pure Chemical Corporation), 0.5 μM CHIR99021 (Selleck Chemicals), 0.5 μM SB431542 (Stemcell Technologies), 5 μM Y27632 (ROCK inhibitor, Selleck Chemicals), 0.8 mM Valproic acid (VPA; Wako Pure Chemical Corporation), 50 ng/mL epidermal growth factor (EGF; PeproTech), and 1.5 μg/mL L-ascorbic acid (Sigma-Aldrich). When the cells were 70 to 80% confluent, they were detached with TrypLE (Gibco) for 10 to 15 min at 37 °C and then the dissociated cells were plated onto collagen IV-coated dishes at 1:3 to 1:5 split ratio. The culture medium was changed every 2 d. All cells were incubated at 37 °C and 5% CO_2. For continuous BMP4 or BAP treatment (*SI Appendix*, Fig. S1 *A* and *B*), PSCs were cultured as previously reported with minor modifications (8, 9). Briefly, PSCs were passaged with ReLeSR and plated on Matrigel-coated plates with mTeSR1 medium. After 1 d, the medium was replaced with 100 ng/mL of human BMP4 (Gibco)-containing MEF-CM (Mouse Embryonic Fibroblast-Conditioned Medium) (8) or BAP (10 ng/mL BMP4, 1 μM A83-01, and 0.1 μM PD173074)-containing DMEM/F12/SR (DMEM/F12 medium supplemented with 20% of KnockOut Serum Replacement [SR]) (9). The cells were cultured for up to 14 d. Media was replaced every day.

Derivation of Stable TSLCs from PSCs. PSCs were dissociated into single cells by using TrypLE and seeded on Matrigel-coated plate (3 to 4 × 10^4 cells/cm^2) containing mTeSR1 medium supplemented with 10 μM Y27632. One day after seeding, the cells were cultured in TSCM containing 10 ng/mL BMP4 for 2 d (for TSLCs) or indicated days as shown in Fig. 1*A*, then they were maintained on Matrigel-coated plates containing TSCM in the absence of BMP4. During the treatment of BMP4, media was changed daily. The cells were passaged every 2 to 3 d with TrypLE when the confluency reached up to 80 to 90% (1:5 to 10 ratio) and analyzed at 14 d or later. All cells were incubated at 37 °C in 5% CO_2.

EVT and ST Differentiation. TSCs and TSLCs were differentiated into EVT and ST as described previously (3). For differentiation of ST, dissociated TSCs and TSLCs were cultured in a 60 mm Petri dish (5 × 10^5 to 1 × 10^6 cells/dish) with 4 mL ST differentiation medium (DMEM/F12 supplemented with 1% ITS-X supplement, 0.5% penicillin-streptomycin, 0.3% BSA, 0.1 mM β-mercaptoethanol, 2.5 μM Y27632, 2 μM forskolin [Selleck Chemicals], and 4% SR). ST differentiation medium was replaced on 3 d. ST derived from TSCs and TSLCs were analyzed on 6 d. For differentiation of EVT, dissociated TSCs and TSLCs were plated on 1 μg/mL collagen IV-coated 6-well plate (1 to 1.5 × 10^4 cells/cm^2) with 2 mL of EVT differentiation medium (DMEM/F12 medium supplemented with 1% ITS-X supplement, 0.5% penicillin-streptomycin, 0.3% BSA, 0.1 mM β-mercaptoethanol, 100 ng/mL human neuregulin-1 [NRG1, Cell Signaling Technology], 7.5 μM A83-01, 2.5 μM Y27632, 4% SR, and 2% Matrigel). On 3 d, the EVT medium was replaced with fresh medium supplemented with reduced Matrigel (0.5%) in the absence of NRG1. On 6 d, the EVT medium was replaced again with the medium containing reduced Matrigel (0.5%) but omitting both NRG1 and SR. EVT derived from TSCs and TSLCs were analyzed on 8 d.

RNA Extraction and RT-qPCR Assay. Total RNA was extracted using the RNeasy plus mini kit (Qiagen) following the manufacturer's instructions and complementary DNAs (cDNAs) were synthesized from 300 to 500 ng of RNAs by qScript cDNA SuperMix (Quantabio). RT-qPCR was performed with PerfeCTa SYBR Green FastMix, Low ROX (Quantabio) and 2 μL of 15 to 20× diluted cDNA. RT-qPCR primer sequences are listed in *SI Appendix*, Table S1. The results were analyzed by ΔΔCt method to calculate fold changes with normalization against glyceraldehyde 3-phosphate dehydrogenase.

RNA Sequencing. To quantify global gene expression, RNA sequencing (RNA-seq) was performed using PSCs, TSLCs, TSCs, and their derivatives. Total RNAs were extracted using the RNeasy plus mini kit following the manufacturer's instructions. RNA-seq libraries were generated with 300 ng of total RNA using NEB Next Ultra II RNA Library prep kit (NEB, E7770) according to the vendor's protocol. Briefly, mRNAs were isolated from total RNAs with Magnetic mRNA Isolation Kit (oligo(dT) beads) (NEB, E7490). First-strand cDNAs were synthesized using random primers and second-strand cDNAs were synthesized subsequently. Double-stranded cDNAs were purified by NEBNext Sample Purification Beads (NEB, E7767), and then the end prep reaction was performed followed by ligation with sample-specific adaptor and index. RNA-seq libraries were sequenced using an Illumina NovasEq. 6000 machine. Paired-end reads from RNA-seq were aligned to the reference human genome (hg38) using STAR (v2.5.2b) (47). For the human genome (hg38), the transcripts information was taken from the GTF file for GRCh38 provided by Gencode (release 35). To generate read counts for each gene, the python package HTSEq. (48) was used. The counts were quantified and normalized by median of ratio method using the R package DESeq2 (v1.32.0) (49). All scripts with details of software versions are freely available from https://

github.com/jyj525/human_TSLC. To obtain EVT- and ST-up-regulated gene sets, we compared the FPKM values between TSCs derived from CT and their derivatives (EVT or ST) from published data (3). Differentially expressed genes were obtained by using limma (v3.48.3) (50) with selection criteria of p-adjusted value < 0.01 and fold change > 2. The PlacentaCellEnrich tool (https://placentacellenrich.gdcb.iastate.edu/) (51) was used to test a significant enrichment of the obtained EVT- and ST-up-regulated gene sets in expected cell type (*SI Appendix*, Fig. S3 *B* and *C* and Tables S5 and S6). For Figs. 3*D* and 4*G*, expression values from all samples were normalized by DESeq2, and violin plots were generated with EVT- and ST-up-regulated gene sets using R software (v4.1.2). Heat maps were generated using Java TreeView (v1.1.6r4) (52) and R software (v4.1.2).

RT-qPCR for miRNAs. For miRNA analysis, total RNAs were isolated using the miRNeasy mini kit (Qiagen) according to the manufacturer's instructions. One microgram of RNAs was converted to cDNAs by using TaqMan MicroRNA Reverse Transcription Kit (Thermo Fisher Scientific). RT-qPCR was conducted with PerfeCTa SYBR Green FastMix, Low ROX. miRNA primer sequences for RT-qPCR are listed in *SI Appendix*, Table S1. The data were analyzed by ΔΔCt method to calculate fold changes with a normalization against miR-103a.

Growth Curve. The TSLCs and TSCs were plated on 96-well plates. Cell Counting Kit-8 (Dojindo Laboratory) was used for a cell proliferation assay. Every 24 h, 10 μL of Cell Counting Kit-8 solution was added to the cultured medium and incubated for 2 h. The absorbance was measured at 450 nm with Infinite M1000 PRO microplate reader (Tecan) for 6 d.

ELISA. The cultured media was collected from ST derived from TSLCs and TSCs on differentiation 6 d. Secretion of hCG was analyzed by ELISA kit for hCG (Ray-Biotech) according to the manufacturer's instructions.

Immunofluorescent Staining. The cells were cultured in a μ-Slide 8 Well chamber (ibidi) for 2 d (TSLCs and TSCs) or 8 d (EVT), and then fixed with 4% paraformaldehyde (PFA; Sigma-Aldrich) for 20 min at room temperature (RT). The ST were cultured for 6 d in Petri dish and collected into 1.5 mL tube. The ST were fixed with 4% PFA for 1 h at RT. The fixed cells were permeabilized and blocked with 0.3% Triton X-100 (Sigma-Aldrich) and 10% normal goat serum (Sigma-Aldrich) in Dulbecco's phosphate-buffered saline (PBS; Thermo Fisher Scientific) for 45 min at RT. For HLA-G staining, a blocking solution was used without 0.3% Triton X-100. The samples were incubated with diluted primary antibodies (*SI Appendix*, Table S2) at 4 °C overnight. The cells were incubated with Alexa Fluor 488- or Alexa Fluor 594-conjugated goat secondary antibodies (1:400; Invitrogen) for 1.5 h at RT. The nuclei of the cells were counterstained with 4′,6-diamidino-2-phenylindole (DAPI; Sigma-Aldrich) for 5 min and the images were acquired using a fluorescence microscope (Zeiss Axiovert, Carl Zeiss).

Bisulfite Sequencing. For extraction of genomic DNA, the cells were resuspended with Tris·HCl (pH 8.0; Sigma-Aldrich), 10 mM ethylenediaminetetraacetic acid (EDTA; Thermo Fisher Scientific), 0.5% sodium dodecyl sulfate (Thermo Fisher Scientific), and 200 μg/mL proteinase K (New England Biolabs) and incubated for 2 h at 55 °C. 0.2 M NaCl was added to the tube. The cell lysates were mixed with PCI (Phenol:Chloroform:Isoamyl Alcohol, Invitrogen) by following manufacturer's instruction and centrifuged with Phase Lock gel (QuantaBio) for 2 min at 12,000 rpm. The supernatant was moved into a new tube and 25 μg/mL ribonuclease A (Life Technologies) was added. The tube was incubated at 37 °C for 1 h. The cells lysates were mixed with PCI and centrifuged with Phase Lock gel again for 2 min at 12,000 rpm. The supernatant was mixed with 2.5× volume of 100% ethanol for precipitation of genomic DNA and centrifuged for 5 min at 12,000 rpm. The genomic DNA was resuspended in 10 mM Tris·HCl, 1 mM EDTA. One microgram of genomic DNA was used for bisulfite conversion by using EpiTect Bisulfite Kit (Qiagen) according to the manufacturer's instructions. Converted DNA was 10× diluted with 10 mM Tris·HCl, 1 mM EDTA. The ELF5 promoter region was amplified using primers as described previously (30). Each PCR product was amplified using EpiMark Hot Start Taq DNA Polymerase (New England Biolabs) following the manufacturer's protocol. The PCR products were purified with a MinElute PCR purification kit (Qiagen) and cloned into qCR2.1 Vector from TA Cloning Kit (Thermo Fisher Scientific) using a molar ratio of 1 plasmid to 2 inserts. After transformation into DH5α competent bacteria, miniprepped DNAs using PureLink Quick Plasmid Miniprep Kit (Invitrogen) were analyzed by Sanger sequencing.

Invasion Assay. The 3D invasion assay was performed by modifying a previously published protocol (32). Molecular Probes Secure Seal Hybridization Chamber (Thermo Scientific) were treated with ultraviolet light for 1 h in a laminar flow hood. The chambers adhered to the bottom of 12-well plate. Matrigel and medium (TSCM or EVT differentiation medium) mix were prepared as 2:1 ratio on ice. Twenty microliters of each Matrigel mix were added to one of the holes in the chamber and equilibrated for 1 h at 37 °C; 5×10^4 cells of TSLCs and TSCs were seeded with 30 μL of TSCM or EVT differentiation medium into another hole of the chamber. To sink the cells to the Matrigel mix, the plate was standing on the side and incubated for 1 h at 37 °C. After then, the chamber was completely covered with 1 mL of additional culture medium. The EVT differentiation was then followed as described in *EVT and ST Differentiation*.

Sodium Fluoresceine (Na-Flu) Leakage Assay. For evaluation of placental barrier function, 5×10^4 cells/cm^2 in 0.1 mL TSCM or ST differentiation medium (detailed information in *Cell Culture* and *EVT and ST Differentiation*) were introduced onto 0.4 μm pore membrane of the apical chamber (Corning, 3470). The basal chamber of the transwell was filled up with 0.6 mL of TSCM or ST differentiation medium. After 3 d and 6 d post seeding, medium of apical chamber was aspirated and transferred to a new 24-well containing 1 mL of PBS for washing. Then, 100 μL of 5 μM Na-Flu in TSCM or ST differentiation medium was added to the apical chamber. The apical chamber was transferred to a new 24-well containing 600 μL of DMEM/F12 medium (without any growth factor supplements) for 1 h in 5% CO_2 at 37 °C. Fifty microliters of samples from the basal chamber were pipetted into a 96-well plate and analyzed using an Infinite M1000 PRO microplate reader (Ex. 460 nm/Em. 515 nm; Tecan). After measurement, the fluorescein solution was aspirated and replaced with TSCM or ST differentiation medium.

Flow Cytometry. EVT cells were differentiated from iPS-TSLCs, ES-TSLCs, and TSCs for 8 d. The cells were dissociated by TrypLE at 37 °C for 30 min and diluted with DMEM/F12. After washing with FACS buffer (PBS without Mg^{2+}, Ca^{2+}, 5% FBS, 2 mM EDTA, and 0.1% sodium azide), the cells were incubated with phycoerythrin-conjugated HLA-G (Abcam) 1:50 diluted in FACS buffer for 30 min on ice. After incubation, the cells were washed 3 times with FACS buffer in the dark. Flow cytometry analysis was performed using a BD Accuri (BD Biosciences) and the data were analyzed using FlowJo software (LLC).

Statistical Analysis. Unless otherwise described, all statistical analyses were performed with three or more biological replicates. Bar chart results were presented as the mean with the SEM. Statistical significance was determined by two-tailed unpaired Student's t-test between two samples or two-way ANOVA for multiple group comparison using R software (v4.1.2) with the annotations: $*P < 0.05$, $**P < 0.01$, and $***P < 0.001$.

Datasets Used for Analysis. We downloaded and analyzed expression data from GSE66302 (human amnion tissues) and the Japanese Genotype-phenotype Archive (JGA) under the accession numbers JGA: JGAD000115 to compare gene expression profile to TSLCs (GSE178162).

Data Availability. Raw and processed RNA-seq data have been deposited to the public server Gene Expression Omnibus (GEO) database under the accession number GSE178162. Previously published data were used for this work GEO (GSE66302 [human amnion tissues] and the JGA under the accession number: JGAD000115).

ACKNOWLEDGMENTS. We thank Drs. Takahiro Arima and Hiroaki Okae (Tohoku University) for sharing human TSC lines and technical advice as well as Dr. Lucy LeBlanc and Christopher Hinds for critical reading of the manuscript. This work was supported by R01HD101512 (NIH/NICHD) and Preterm Birth Research Grant (1017294, Burroughs Wellcome Fund) to J.K.

1. R. M. Lewis, J. K. Cleal, M. A. Hanson, Review: Placenta, evolution and lifelong health. *Placenta* **33** (suppl.), S28–S32 (2012).

2. A. E. Guttmacher, Y. T. Maddox, C. Y. Spong, The Human Placenta Project: Placental structure, development, and function in real time. *Placenta* **35**, 303–304 (2014).

3. H. Okae *et al.*, Derivation of human trophoblast stem cells. *Cell Stem Cell* **22**, 50–63.e6 (2018).
4. S. J. Fisher, The placental problem: Linking abnormal cytotrophoblast differentiation to the maternal symptoms of preeclampsia. *Reprod. Biol. Endocrinol.* **2**, 53 (2004).
5. M. Lacroix, E. Kina, M.-F. Hivert, Maternal/fetal determinants of insulin resistance in women during pregnancy and in offspring over life. *Curr. Diab. Rep.* **13**, 238–244 (2013).
6. S. J. Heaton *et al.*, The use of BeWo cells as an in vitro model for placental iron transport. *Am. J. Physiol. Cell Physiol.* **295**, C1445–C1453 (2008).
7. H. G. Frank *et al.*, Cytogenetic and DNA-fingerprint characterization of choriocarcinoma cell lines and a trophoblast/choriocarcinoma cell hybrid. *Cancer Genet. Cytogenet.* **116**, 16–22 (2000).
8. R.-H. Xu *et al.*, BMP4 initiates human embryonic stem cell differentiation to trophoblast. *Nat. Biotechnol.* **20**, 1261–1264 (2002).
9. M. Amita *et al.*, Complete and unidirectional conversion of human embryonic stem cells to trophoblast by BMP4. *Proc. Natl. Acad. Sci. U.S.A.* **110**, E1212–E1221 (2013).
10. M. Horii *et al.*, Human pluripotent stem cells as a model of trophoblast differentiation in both normal development and disease. *Proc. Natl. Acad. Sci. U.S.A.* **113**, E3882–E3891 (2016).
11. Y. Li, M. M. Parast, BMP4 regulation of human trophoblast development. *Int. J. Dev. Biol.* **58**, 239–246 (2014).
12. R. M. Roberts, T. Ezashi, M. A. Sheridan, Y. Yang, Specification of trophoblast from embryonic stem cells exposed to BMP4. *Biol. Reprod.* **99**, 212–224 (2018).
13. A. S. Bernardo *et al.*, BRACHYURY and CDX2 mediate BMP-induced differentiation of human and mouse pluripotent stem cells into embryonic and extraembryonic lineages. *Cell Stem Cell* **9**, 144–155 (2011).
14. G. Guo *et al.*, Human naive epiblast cells possess unrestricted lineage potential. *Cell Stem Cell* **28**, 1040–1056.e6 (2021).
15. S. Io *et al.*, Capturing human trophoblast development with naive pluripotent stem cells in vitro. *Cell Stem Cell* **28**, 1023–1039.e13 (2021).
16. T. Ezashi, B. P. Telugu, R. M. Roberts, Model systems for studying trophoblast differentiation from human pluripotent stem cells. *Cell Tissue Res.* **349**, 809–824 (2012).
17. R. M. Roberts *et al.*, Differentiation of trophoblast cells from human embryonic stem cells: To be or not to be? *Reproduction* **147**, D1–D12 (2014).
18. X. Gao *et al.*, Establishment of porcine and human expanded potential stem cells. *Nat. Cell Biol.* **21**, 687–699 (2019).
19. Z. Li, O. Kurosawa, H. Iwata, Establishment of human trophoblast stem cells from human induced pluripotent stem cell-derived cystic cells under micromesh culture. *Stem Cell Res. Ther.* **10**, 245 (2019).
20. C. Dong *et al.*, Derivation of trophoblast stem cells from naïve human pluripotent stem cells. *eLife* **9**, e52504 (2020).
21. J. K. Cinkornpumin *et al.*, Naive human embryonic stem cells can give rise to cells with a trophoblast-like transcriptome and methylome. *Stem Cell Reports* **15**, 198–213 (2020).
22. Y. Wei *et al.*, Efficient derivation of human trophoblast stem cells from primed pluripotent stem cells. *Sci. Adv.* **7**, eabf4416 (2021).
23. A. Mischler *et al.*, Two distinct trophectoderm lineage stem cells from human pluripotent stem cells. *J. Biol. Chem.* **296**, 100386 (2021).
24. S. Yabe *et al.*, Comparison of syncytiotrophoblast generated from human embryonic stem cells and from term placentas. *Proc. Natl. Acad. Sci. U.S.A.* **113**, E2598–E2607 (2016).
25. T. Faial *et al.*, Brachyury and SMAD signalling collaboratively orchestrate distinct mesoderm and endoderm gene regulatory networks in differentiating human embryonic stem cells. *Development* **142**, 2121–2135 (2015).
26. M. S. Roost *et al.*, KeyGenes, a tool to probe tissue differentiation using a human fetal transcriptional atlas. *Stem Cell Reports* **4**, 1112–1124 (2015).
27. Y. Shao *et al.*, Self-organized amniogenesis by human pluripotent stem cells in a biomimetic implantation-like niche. *Nat. Mater.* **16**, 419–425 (2017).
28. R. C. V. Tyser *et al.*, Single-cell transcriptomic characterization of a gastrulating human embryo. *Nature* **600**, 285–289 (2021).
29. Y. Yang *et al.*, Heightened potency of human pluripotent stem cell lines created by transient BMP4 exposure. *Proc. Natl. Acad. Sci. U.S.A.* **112**, E2337–E2346 (2015).
30. C. Q. Lee *et al.*, What is trophoblast? A combination of criteria define human first-trimester trophoblast. *Stem Cell Reports* **6**, 257–272 (2016).
31. J. Kim *et al.*, A Myc network accounts for similarities between embryonic stem and cancer cell transcription programs. *Cell* **143**, 313–324 (2010).
32. K. J. Bayless, H. I. Kwak, S. C. Su, Investigating endothelial invasion and sprouting behavior in three-dimensional collagen matrices. *Nat. Protoc.* **4**, 1888–1898 (2009).
33. J.-L. Frendo *et al.*, Direct involvement of HERV-W Env glycoprotein in human trophoblast cell fusion and differentiation. *Mol. Cell. Biol.* **23**, 3566–3574 (2003).
34. V. Jokimaa *et al.*, Expression of syndecan-1 in human placenta and decidua. *Placenta* **19**, 157–163 (1998).
35. T. Fournier, Human chorionic gonadotropin: Different glycoforms and biological activity depending on its source of production. *Ann. Endocrinol. (Paris)* **77**, 75–81 (2016).
36. M. Rothbauer *et al.*, A comparative study of five physiological key parameters between four different human trophoblast-derived cell lines. *Sci. Rep.* **7**, 5892 (2017).
37. M. Tomi, T. Nishimura, E. Nakashima, Mother-to-fetus transfer of antiviral drugs and the involvement of transporters at the placental barrier. *J. Pharm. Sci.* **100**, 3708–3718 (2011).
38. B. J. Cox, "Systems biology analyses of the placenta" in *The Guide to Investigation of Mouse Pregnancy*, A. Croy, A. T. Yamada, F. J. DeMayo, S. L. Adamson, Eds. (Academic Press, 2014), pp. 259–274.
39. M. Iqbal, M. C. Audette, S. Petropoulos, W. Gibb, S. G. Matthews, Placental drug transporters and their role in fetal protection. *Placenta* **33**, 137–142 (2012).
40. M. V. St-Pierre *et al.*, Expression of members of the multidrug resistance protein family in human term placenta. *Am. J. Physiol. Regul. Integr. Comp. Physiol.* **279**, R1495–R1503 (2000).
41. M. Nishimura, S. Naito, Tissue-specific mRNA expression profiles of human ATP-binding cassette and solute carrier transporter superfamilies. *Drug Metab. Pharmacokinet.* **20**, 452–477 (2005).
42. P. Myllynen, K. Vähäkangas, Placental transfer and metabolism: An overview of the experimental models utilizing human placental tissue. *Toxicol. In Vitro* **27**, 507–512 (2013).
43. G. Castel *et al.*, Induction of human trophoblast stem cells from somatic cells and pluripotent stem cells. *Cell Rep.* **33**, 108419 (2020).
44. X. Liu *et al.*, Reprogramming roadmap reveals route to human induced trophoblast stem cells. *Nature* **586**, 101–107 (2020).
45. K. Benirschke, G. J. Burton, R. N. Baergen, "Basic structure of the villous trees" in *Pathology of the Human Placenta* (Springer-Verlag Berlin Heidelberg, 2012), pp. 55–100.
46. C. Han *et al.*, Syncytiotrophoblast-derived extracellular vesicles in pathophysiology of preeclampsia. *Front. Physiol.* **10**, 1236 (2019).
47. A. Dobin *et al.*, STAR: Ultrafast universal RNA-seq aligner. *Bioinformatics* **29**, 15–21 (2013).
48. S. Anders, P. T. Pyl, W. Huber, HTSeq–A Python framework to work with high-throughput sequencing data. *Bioinformatics* **31**, 166–169 (2015).
49. M. I. Love, W. Huber, S. Anders, Moderated estimation of fold change and dispersion for RNA-seq data with DESeq2. *Genome Biol.* **15**, 550 (2014).
50. M. E. Ritchie *et al.*, limma powers differential expression analyses for RNA-sequencing and microarray studies. *Nucleic Acids Res.* **43**, e47 (2015).
51. A. Jain, G. Tuteja, PlacentaCellEnrich: A tool to characterize gene sets using placenta cell-specific gene enrichment analysis. *Placenta* **103**, 164–171 (2021).
52. A. J. Saldanha, Java Treeview–Extensible visualization of microarray data. *Bioinformatics* **20**, 3246–3248 (2004).